THE ASTROPHYSICAL JOURNAL, 558:L55–L58, 2001 September 1

THE RELATIONSHIP BETWEEN THE CIRCULAR POLARIZATION AND THE MAGNETIC FIELD FOR ASTROPHYSICAL MASERS WITH WEAK ZEEMAN SPLITTING

W. D. WATSON AND H. W. WYLD
Department of Physics, University of Illinois at Urbana-Champaign, 1110 West Green Street, Urbana, IL 61801-3080
Received 2001 June 27; accepted 2001 July 27; published 2001 August 3

ABSTRACT

The relationship between the magnetic field and the circular polarization of astrophysical maser radiation due to the Zeeman effect under idealized conditions is investigated when the Zeeman splitting is much smaller than the spectral line breadth and when radiative saturation is significant. The description of the circular polarization as well as inferences about the magnetic field from the observations are clearest when the rate for stimulated emission is much less than the Zeeman splitting. The calculations here are performed in this regime, which is relevant for some (if not most) observations of astrophysical masers. We demonstrate that the Stokes *V* parameter is proportional to the Zeeman splitting and that the fractional linear polarization is independent of the Zeeman splitting when the ratio of the Zeeman splitting to the spectral line breadth is small—less than about 0.1. In contrast to its behavior for ordinary spectral lines, the circular polarization for masers that are at least partially saturated does not decrease with increasing angle between the magnetic field and the line of sight until they are nearly perpendicular.

Subject headings: magnetic fields — masers — polarization

1. INTRODUCTION

The circular polarization of maser radiation in which the Zeeman splitting is much smaller than the spectral line breadth is utilized in efforts to obtain information about the magnetic field in various astronomical contexts (e.g., for recent work, see Kemball & Diamond 1997, Sarma, Troland, & Romney 2001, Vlemmings, Diamond, & van Langevelde 2001, and Yusef-Zadeh et al. 1999). For a two-level, nonmasing ("thermal") spectral line, a simple relationship exists,

$$V/(\partial I/\partial v) = pB\cos\theta, \tag{1}$$

that involves the Stokes *V* parameter, the derivative of the intensity *I* with respect to Doppler velocity *v*, the magnetic field *B*, and the angle θ between the magnetic field and the line of sight (*p* is a constant of the molecular physics for the specific transition). When maser saturation is unimportant, the relationship can readily be seen as applicable for masers as well (e.g., Fiebig & Gusten 1989). Although maser polarization in the presence of saturation was the focus of the classic investigation by Goldreich, Keeley, & Kwan (1973, hereafter GKK), they provide no guidance on the circular polarization for weak Zeeman splitting. GKK only consider the line center, where the circular polarization is zero in the weak splitting regime. For a summary of the theory of maser polarization, see Watson (2001).

The GKK idealization is a uniformly pumped, linear maser in a steady state. The seed radiation is external, weak continuum radiation, and the masing involves an angular momentum $J = 1$–0 transition in the presence of a constant magnetic field. Even though the actual circumstances may be more complicated, the idealization and solutions of GKK have served as the basis for discussions of maser polarization in general. In this Letter, we partially remedy the omission of GKK for weak splitting by calculating the Stokes *V* parameter for this basic idealization in the limit that the rate *R* for stimulated emission is much less than the Zeeman splitting $g\Omega$ (where $\Omega = eB/m_e c$ and *g* is the Lande *g*-factor). This limit certainly is applicable when $g\Omega$ is a noticeable fraction (greater than a few percent) of the line width, as occurs for the 1720 MHz OH masers. It probably also is relevant for the 22 GHz water masers for which $g\Omega \simeq 10^4 B(G)\ \mathrm{s}^{-1}$ for the $F = 7$–6 transition and provides at least a basis for discussion for the SiO masers for which $g\Omega \simeq 10^3 B(G)\ \mathrm{s}^{-1}$. As a benchmark, the measure of the degree of saturation is the ratio of *R* to the loss rate Γ that ordinarily is taken to be about 1 and 5 s^{-1} for the H_2O and SiO masers, respectively, and somewhat less for the 1720 MHz masers. We limit our attention to $g\Omega \gg R$ because here the modifications to the standard Zeeman effect are moderate and the magnetic field can still be inferred from the Stokes *V* parameter with some confidence. Both the conceptualization and the calculation of the Stokes *V* parameter are considerably simpler in this regime because only "ordinary rate equations" and "ordinary molecular populations" of the magnetic substates are involved. In contrast, when $g\Omega \gg R$ is not satisfied, the Stokes *V* parameter can be much larger (sometimes referred to as "non-Zeeman" effects) than expected from the standard Zeeman relationship (Nedoluha & Watson 1994). It is unclear whether useful information about the magnetic field can be inferred from the observations in this regime. The more involved methods of the quantum mechanical density matrix must be utilized in this regime to incorporate the correlations between the magnetic substates. Large, non-Zeeman circular polarization can also be generated by effects that would not be present in the GKK idealization for masing, such as changes in the direction of the magnetic field within the masing region (Wiebe & Watson 1998).

Calculations of the type being presented here have previously been performed (Nedoluha & Watson 1992), but only for a quite limited range of saturation and angles θ, and only for the molecular parameters that are specific to the 22 GHz masing transition, i.e., for the high angular momenta ($F = 7$, 6, 5, and 4) and when the values of the magnetic moments are different for the upper and lower molecular states. These calculations did demonstrate that maser saturation alters equation (1) and that its effect is to increase the Stokes *V* parameter much more at large angles than at small angles relative to that expected from equation (1). The latter is especially significant because lines of sight to masers are often likely to be nearly perpendicular to the magnetic fields (e.g., toward circumstellar masing rings, toward the centers of accretion disks viewed edge-on). The intent of this Letter is to provide a comprehensive description of the relation-

ship between the circular polarization and the magnetic field within the limitations outlined above and to do this for the idealized masing conditions treated by GKK that have served as a basis for discussing maser polarization.

2. CALCULATIONS

The rate equations for the normalized (dimensionless) population differences n_+, n_-, and n_0 between the magnetic substates $m = +1$, -1, and 0 of the upper (angular momentum $J = 1$) energy level and the $m = 0$ substate of the lower ($J = 0$) level, respectively, are functions of the molecular velocity v and can be expressed by (e.g., Wallin & Watson 1995; see also GKK)

$$1 = (1 + 2R_+)n_+ + R_0 n_0 + R_- n_- \tag{2}$$

and the two related equations that are obtained by exchanging the $\pm$ and 0 indexes in equation (2). "Phenomenological" pumping and loss rates "Λ" and "Γ," which are standard in maser theory, have been utilized and incorporated into the normalizations of the populations to obtain equation (2). For a unidirectional linear maser, the normalized rates for stimulated emission in equation (2) are

$$R_\pm = I_\pm(1 + \cos^2\theta) + Q_\pm \sin^2\theta \pm 2V_\pm \cos\theta, \tag{3}$$

$$R_0 = 2(I_0 - Q_0)\sin^2\theta, \tag{4}$$

where the subscripts $\pm$ and 0 indicate that the intensities are to be evaluated at the frequencies (angular) $\omega_\pm$ and ω_0 for which

$$(1 - v/c)\omega_\pm = \omega_R \pm g\Omega/2, \tag{5}$$

$$(1 - v/c)\omega_0 = \omega_R. \tag{6}$$

Here ω_R is the resonance frequency of the transition and $\pm g\Omega/2$ are the Zeeman shifts of the $m = \pm 1$ magnetic substates. The dimensionless Stokes intensities (I, Q, and V) are actual intensities divided by the characteristic saturation intensity $I_S = (8\hbar\omega^3\Gamma/3\pi c^2 A_E)$, where A_E is the Einstein A-value for the transition. Note that whereas $R_\pm$ and R_0 are dimensionless, R itself is not normalized and retains its usual dimensions (time^{-1}) in our discussions. The radiative transfer equations

$$dI/ds = AI + BQ + CV, \tag{7}$$

$$dQ/ds = AQ + BI, \tag{8}$$

$$dV/ds = AV + CI \tag{9}$$

are at a specific frequency ω and can be solved numerically as a function of the normalized distance s with the expressions

$$A = (1 + \cos^2\theta)(f_+ n_+ + f_- n_-) + 2f_0 n_0 \sin^2\theta, \tag{10}$$

$$B = \sin^2\theta(f_+ n_+ + f_- n_- - 2f_0 n_0), \tag{11}$$

$$C = 2\cos\theta(f_+ n_+ - f_- n_-), \tag{12}$$

where the f's are Maxwellian distributions for the component of the velocity that is along the path of the radiation. In these equations, $f_\pm$, $n_\pm$, f_0, and n_0 are evaluated at velocities $v_\pm$ and v_0 given by $(1 - v_\pm/c)\omega = \omega_R \pm g\Omega/2$ and $(1 - v_0/c)\omega = \omega_R$.

Starting from the initial conditions $I \ll 1$ and $Q = 0 = V$, the radiative transfer equations are integrated numerically at a sufficient number of frequencies ω to delineate the profile of the spectral line. We emphasize that the foregoing equations are valid only when $g\Omega \gg R$. They are the same as would describe the polarization of ordinary thermal radiation—the only differences being the sign of the net pumping rate that is reflected in the sign of the "1" on the left-hand side of equation (2) and the ignoring of spontaneous emission.

The main results are presented in the Figure 1 in terms of the ratios $V/(pB\partial I/\partial v)$ and Q/I computed for a value of $g\Omega$ that is much less than the spectral line breadth and at a frequency that is essentially (although not exactly) at line center. These ratios are useful because, in the weak splitting regime and consistent with equation (1), they tend to be independent of $g\Omega$ and constant with frequency across the spectral line. At frequencies where the bulk of the intensity occurs, we have confirmed that the ratios in Figure 1 are independent of frequency to a good approximation in the weak splitting regime as delineated in the following paragraph. Exceptions to this generalization do occur at the angles for which the deviations from equation (1) are greatest when the intensities are in the neighborhood of $I = 1$. Where there are variations in $V/(pB\partial I/\partial v)$ and Q/I with frequency, these variations are modest and are smallest near line center. Note that the properties of the radiation at different frequencies within the spectral line are not completely independent because of the coupling that is indicated in equations (5) and (6) and in the analogous expressions for $v_\pm$ and v_0. In detail, the rate for stimulated emission depends on the polarization of the radiation and on the angle θ and is not exactly the same for all of the magnetic substates. It nevertheless is useful to utilize I (which is normalized by the characteristic saturation intensity) as the measure of the degree of saturation. That is, $I \simeq R/\Gamma$.

The goal here is limited to providing information on the polarization characteristics for the limit of weak Zeeman splitting—that is, for small enough $g\Omega$ that the ratios in Figure 1 are independent of $g\Omega$ to a good approximation for the bulk of the radiation within the spectral line. The precise accuracy of this approximation for a specific $g\Omega$ depends on angle θ, the degree of saturation, and the Doppler velocity within the spectral line and is not exactly the same for the linear and the circular polarization. Nevertheless, some useful generalizations can be made. We compute polarizations for $g\Omega$ as large as one-fifth of the FWHM thermal Doppler breadth $\Delta\omega_t$ [$\Delta\omega_t = 2.4\omega_R\,(kT/Mc^2)^{1/2}$]. As long as the degree of saturation is greater than one, the ratios presented in Figure 1 are independent of $g\Omega$ to an accuracy of a few percent. Likewise, as long as $g\Omega/\Delta\omega_t \leq 0.05$, these ratios also are independent of $g\Omega$ to a similar accuracy regardless of the degree of saturation. For lower saturations—I down to 0.01—and $0.2 \geq g\Omega/\Delta\omega_t \geq 0.05$,

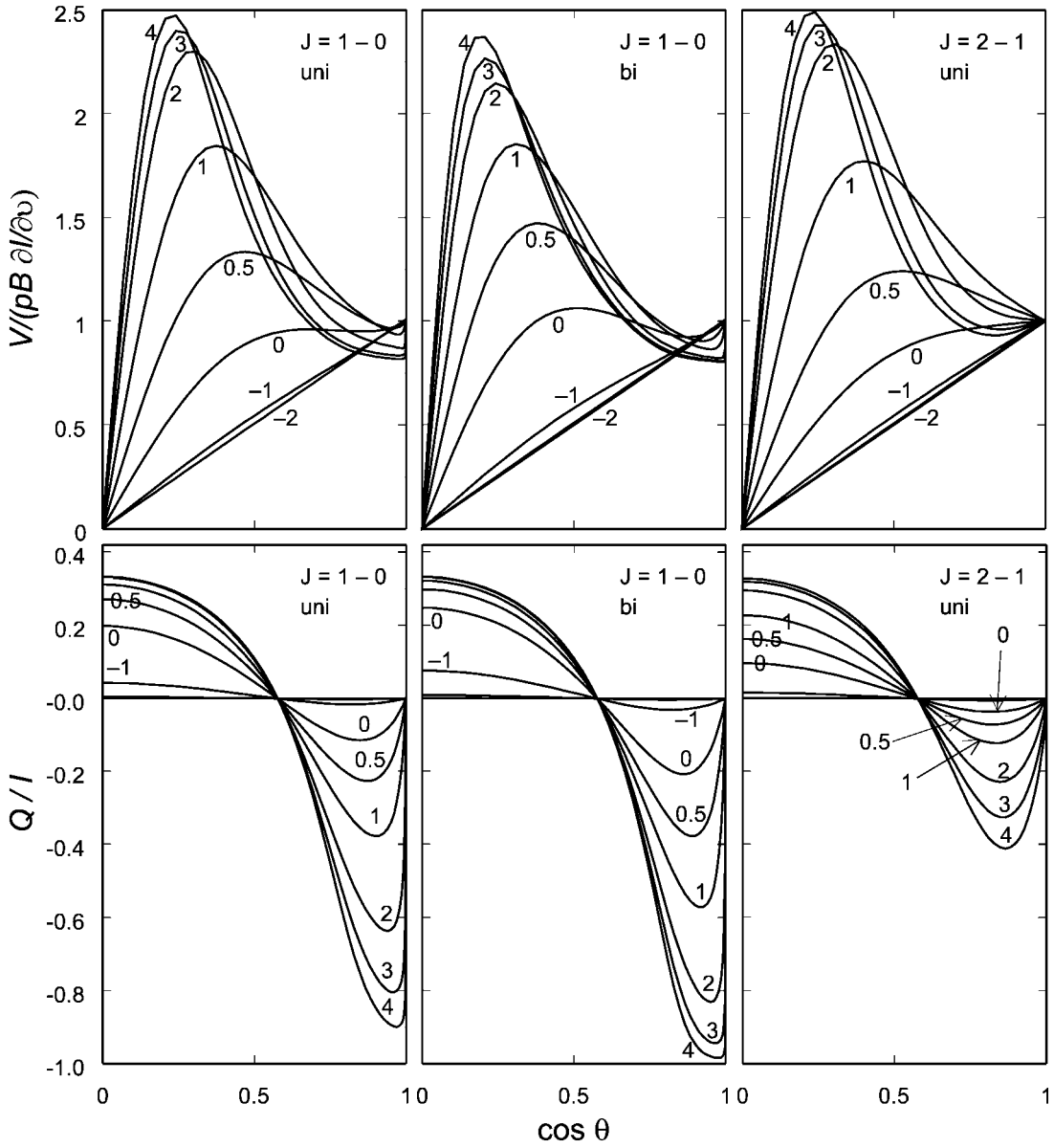

FIG. 1.—Circular and linear polarization of maser radiation as a function of the cosine of the angle θ between the direction of the magnetic field and the line of sight. Polarizations are presented for $J = 1$–0 unidirectional and bidirectional masers and for $J = 2$–1 unidirectional masers in separate panels as indicated by the label in each panel. The curves are labeled by the log of the intensity I, which is essentially the degree of saturation. Curves (some of which overlap) are plotted for $I = 10^{-2}$, 10^{-1}, 1, 3, 10, 10^2, 10^3, and 10^4. *Upper three panels*: Circular polarization as measured by the magnitude of $V/(pB\partial I/\partial v)$, which is equal to $\cos\theta$ in the unsaturated limit. *Lower three panels*: Fractional linear polarization. The Stokes Q parameter is positive when the linear polarization is perpendicular to the direction of the magnetic field projected onto the plane of the sky.

the ratio $V/(pB\partial I/\partial v)$ is still independent of $g\Omega$ to within about 20% accuracy. The main deviations occur at angles less than about 45° where the effects of saturation are the least.

The main effect of saturation on the circular polarization is readily evident in Figure 1. Instead of decreasing as $\cos\theta$ when the angle θ increases from zero, the Stokes V parameter tends to increase until a relatively large angle is reached whose value is determined by the exact degree of saturation. At $\theta = 0$, the Stokes V parameter becomes equal to its value for unsaturated masing. The nearly discontinuous change reflects the change in the molecular populations that is associated with the similarly rapid variation of the linear polarization as θ approaches zero in the GKK theory. The variation of the linear polarization with saturation can be sensitive to the angular momentum of the molecular states (e.g., Deguchi & Watson 1990). We have thus performed similar calculations for a $J = 2$–1 masing transition as well, with the idealization that g is the same for the upper and lower energy levels (hence, $p = ge/2m_e\omega_R$ is the same for both transitions). These also are presented in Figure 1, along with additional results from a further calculation in which the $J = 1$–0 masing is treated as bidirectional. The optical depths are the same for radiation propagating in opposite directions in a linear maser. If the external seed radiation is similar at both ends of the maser (or if the seed radiation is due to spontaneous emission), the radiation propagating in the two directions will also be similar, and the maser will be "bidirectional." It is known that the variation of the linear polarization with saturation can be different for uni- and bidirectional masers (Western & Watson 1984). However, the comparisons in Figure 1 demonstrate that the differences for the circular polari-

zation are small for both of these modifications that we have considered beyond the basic unidirectional $J = 1$–0 maser.

The fractional linear polarization in Figure 1 is identical to that obtained in previous calculations. We present it here in the same format as the circular polarization for convenience in relating the two polarizations. At high saturation, the fractional linear polarizations in our calculations (see also Western & Watson 1984) do reach those of GKK—which are obtained by GKK only for the limit of high saturation. The fractional linear polarization is seen in Figure 1 to increase more rapidly as a function of saturation for $J = 1$–0 than for $J = 2$–1 masers and more rapidly for bidirectional than for unidirectional masers. However, for the polarization to reach the very highest Q/I given by GKK, the degree of saturation must be implausibly high for $J = 2$–1 masers—as found previously. Anisotropic (or "*m*-dependent") pumping by starlight is thus the most likely cause for the highest fractional linear polarizations of the SiO and perhaps other masers (Western & Watson 1983).

Unfortunately, the degree of radiative saturation of astrophysical masers is a long-standing uncertainty. In addition to the surface brightness of the maser, the saturation depends on the angle into which the radiation is beamed—a quantity for which direct estimates ordinarily are unreliable (e.g., Watson & Wyld 2000). Note that the "intensities" of the linear maser formulation (by us and by GKK) actually are "mean intensities" times 4π. Hence, intensities from the observations must be multiplied by the solid angle of the beam (as well as divided by I_S) in order to relate them to the I in the figures. A comparison of the observed linear polarization with that in Figure 1 can be helpful to restrict the degree of saturation if there are no contaminating effects such as anisotropic pumping, multiple components, or Faraday rotation. The narrowing of the spectral line during unsaturated maser amplification, followed by rebroadening of the line when the maser becomes saturated, can also be used to obtain an indication of saturation (e.g., Nedoluha & Watson 1991) if there are no velocity gradients or multiple components within the maser. A consideration of the line breadths of certain prominent 22 GHz water masers indicates that the influence of saturation on the Stokes V parameter is probably modest for these masers (Nedoluha & Watson 1992). The line breadth in our calculations is given in Figure 2 as a function of I. It does depend somewhat on the intensity of the incident continuum seed radiation. The computations in Figure 1 are performed for an incident intensity $I = 10^{-9}$ that we believe to be representative. We have also performed computations analogous to those in Figure 1 when the incident intensity I is 10^{-5}, as might occur when the masing gas is amplifying a strong continuum source. The resulting Q/I ratios are essentially identical to those in Figure 1. The Stokes V parameters also are quite similar to those in Figure 1, except near the peaks of the curves for the largest I ($\gtrsim 10^2$) where they are smaller by 15%–20%.

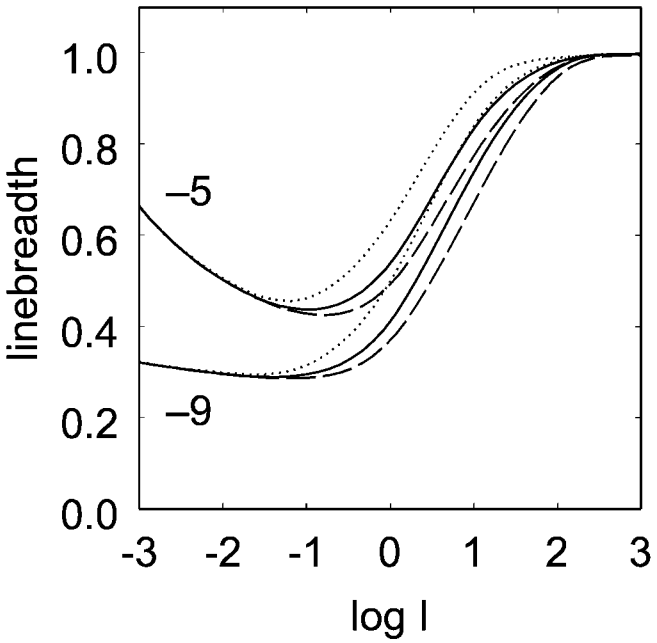

FIG. 2.—Ratio of the spectral line breadth (FWHM) of the maser radiation to the Doppler breadth $\Delta\omega_t$ (FWHM) of the thermal velocities of the masing molecules, as a function of the log of the intensity I. Line breadths are shown for $J = 1$–0 unidirectional (*solid lines*), $J = 1$–0 bidirectional (*dotted lines*), and $J = 2$–1 unidirectional (*dashed lines*) masers with intensities for the incident continuum radiation of $I = 10^{-5}$ as well as for $I = 10^{-9}$, which we consider to be most representative.

In summary, when the observed masers are believed to be at least somewhat saturated, but when there is no good information about the angle θ or about the exact degree of saturation, simply removing the $\cos\theta$ in equation (1) would seem to provide the best way at present to infer magnetic field strengths from the observed the Stokes V parameter in the weak splitting regime when "non-Zeeman effects" can be ignored. Saturation with $I \gtrsim 10^2$ (and probably even $I \gtrsim 10$) seems unlikely for astrophysical masers. In contrast to the linear polarization, the circular polarization is relatively insensitive to the angular momentum of the molecular states. We emphasize that our results are applicable in detail only to the idealized masing conditions on which the calculations are based (see § 1). In addition to non-Zeeman effects, velocity gradients, anisotropic pumping, and multiple hyperfine components may be present but are not considered here. For example, the 22 GHz masing transition of water probably consists of multiple hyperfine components, and so equation (1) is unlikely to be directly applicable (but see Nedoluha & Watson 1992).

This research has been supported in part by NSF grant AST 99-88104.

REFERENCES

Deguchi, S., & Watson, W. D. 1990, ApJ, 354, 649
Fiebig, D., & Gusten, R. 1989, A&A, 214, 333
Goldreich, P., Keeley, D. S., & Kwan, J. Y. 1973, ApJ, 179, 111 (GKK)
Kemball, A. J., & Diamond, P. J. 1997, ApJ, 481, L111
Nedoluha, G. E., & Watson, W. D. 1991, ApJ, 367, L63
———. 1992, ApJ, 384, 185
———. 1994, ApJ, 423, 394
Sarma, A. P., Troland, T. H., & Romney, J. D. 2001, ApJ, 554, L217
Vlemmings, W., Diamond, P. J., & van Langevelde, H. J. 2001, in IAU Symp. 206, Cosmic Masers: From Protostars to Black Holes, ed. V. Migenes & E. Ludke (San Francisco: ASP), in press
Wallin, B. K., & Watson, W. D. 1995, ApJ, 445, 465
Watson, W. D. 2001, in IAU Symp. 206, Cosmic Masers: From Protostars to Black Holes, ed. V. Migenes & E. Ludke (San Francisco: ASP), in press
Watson, W. D., & Wyld, H. W. 2000, ApJ, 530, 207
Western, L. R., & Watson, W. D. 1983, ApJ, 275, 195
Western, L. R., & Watson, W. D. 1984, ApJ, 285, 158
Wiebe, D. S., & Watson, W. D. 1998, ApJ, 503, L71
Yusef-Zadeh, F., Roberts, D. A., Goss, W. M., Frail, D. A., & Green, A. J. 1999, ApJ, 512, 230